Proceedings of the ASME 27th International Conference on Offshore Mechanics and Arctic Engineering
OMAE 2008
June 15-20, 2008, Estoril, Portugal

OMAE2008-57793

ELASTODYNAMIC ANALYSIS OF TOWED CABLE SYSTEMS BY GLOBAL NODAL POSITION VECTOR FINITE ELEMENT METHOD

Zheng H. Zhu*
York University
Dept. of Earth and Space Science and Engineering
4700 Keele Street, Toronto, Ontario, M3J 1P3, Canada
Email: gzhu@yorku.ca

Michael LaRosa
Curtiss-Wright Controls
Engineered Systems - Marine Defense
3570 Hawkestone Rd, Mississauga, ON, L5C 2V8, Canada
Email: Michael_LaRosa@indaltech.com

Feng J. Sun
York University
Dept. of Earth and Space Science and Engineering
4700 Keele Street, Toronto, Ontario, M3J 1P3, Canada
Email: fengjing@yorku.ca

ABSTRACT

The handling and control of towed cable and body systems onboard surface ships and submarines presents a significant technical challenge to design engineers in the defense and ocean industries. The current approaches rely heavily on the empirical methods and the time-consuming and costly prototype testing. Computer simulation provides a cost effective way to reduce the high risks associated with the towed cable/body system. However, the current dynamic analysis of towed cables is mostly done by the finite difference (FD) method in stead of the finite element (FE) method that is widely used in almost all engineering fields. This paper presents an alternative FE method to simulate the dynamics of towed cable and body system, in which the large rigid body motion is coupled with small elastic deformation. The newly derived FE method is formulated in terms of element nodal positions, which is different from the existing FE methods that use displacements. The alternative FE method solves for the cable position directly in order to eliminate accumulated numerical errors arising from existing FE methods that solve for displacements first in order to obtain the cable position over very long period of time. The alternative FE formulation is implemented and applied to real applications to demonstrate its robustness by comparing simulation results with the experimental and sea trial data.

1. INTRODUCTION

Towed cable systems have a wide range of applications in science, industry, and defense. Examples of such systems include underwater mooring lines [1], towed sonar array and remote operated vehicles [2], aerial refueling hose and drogue [3], and tethered satellites [4], just to name a few. The cable is usually simplified as a flexible tension member and its bending stiffness is neglected because of the extremely large ratio of length over cross-section dimension [5]. The motion of the towed cable usually involves large rigid body motion and small elastic stretch. Linear cable theory is usually not adequate and the nonlinear geometric stiffness of the cable should be included to account for the geometric nonlinearity due to the large displacements and rotations experienced by the cable. Generally speaking, the dynamic analysis of the towed cable systems can be grouped into four categories: 1) analytical, 2) lumped parameter, 3) finite difference (FD), and 4) finite element (FE) method, respectively.

The analytical solutions are only available in limited cases involving grossly simplified assumptions, such as the description of the steady state solution for a string [6]. The lumped parameter method simplifies the coupled nonlinear partial differential equations of motion into ordinary differential equations by lumping the distributed mass, external loads, inertia forces of the cable to specified nodes along the cable [7]. The finite difference method approximates the governing equations of a cable by some difference equations along the cable [8]. Solutions of the cable dynamics using FD

* Assistant Professor and author of correspondence

and lumped parameter methods are very popular and are predominant in the dynamic analysis of cable systems because of their mathematic simplicity; see the works of Burgess [9] and other researchers [10]. However, the FD and lumped parameter methods are problem specific and are not easy to be implemented in general-purpose analysis programs for complex geometries with multiple cable branches or different cable properties along the length. In the finite element method, the continuous cable is discretized into a finite number of elements. Each finite element may have different cable properties but the governing mathematic equations for each element are the same. By assembling all the elements together, the complex geometries with multiple cable branches or different cable properties along the length can be easily modeled algorithmically [5]. The FE method is probably the most appealing technique among all engineering numerical methods. The main advantage of FE over FD is its capability in handling the complex cable systems in an algorithmic fashion, allowing for its implementation in general-purpose analysis programs. However, the FE method has not yet been widely used in the dynamic modeling of towed cables compared with FD.

The main reason that limits the FE application in cable dynamic analysis is that the towed cables usually experience very large rigid body motion and extremely small elastic stretch. The main interest in cable dynamic analysis is its position. The FD method formulates the cable dynamics in terms of its position directly while the existing FE methods solve for cable displacement first and then the new position of cable by adding the displacement to the old position. Because the large rigid body rotation of the cable leads to geometrical nonlinearity, improper approximation in calculating the strain of element based on displacement approach will result in numerical errors that do not exist in FD method, where the strain is calculated by comparing the current configuration with original configuration directly. For instance, let's consider a planer cable element experiencing a rigid body rotation as shown in Fig. 1. The displacements of the element can be expressed as:

$$u = u_1 + x(\cos\theta - 1), \qquad v = v_1 + x\sin\theta \tag{1}$$

The Green-Lagrangian strain of the element is defined as [11]:

$$\varepsilon_x = \frac{\partial u}{\partial x} + \frac{1}{2}\left[\left(\frac{\partial u}{\partial x}\right)^2 + \left(\frac{\partial v}{\partial x}\right)^2\right] \tag{2}$$

Since the rigid body rotation of the cable element does not cause any deformation, the strain of the element should be zero. This is evident by substituting Eq. (1) into Eq. (2), such that:

$$\varepsilon_x = \cos\theta - 1 + \frac{1}{2}\left[(\cos\theta - 1)^2 + \sin^2\theta\right] = 0$$

The commonly used approximation in FE methods for the nonlinear strain expression in Eq. (2) can be written as, if the strain is small,

$$\hat{\varepsilon}_x = \frac{\partial u}{\partial x} + \frac{1}{2}\left(\frac{\partial v}{\partial x}\right)^2 \tag{3}$$

Substituting Eq. (1) into Eq. (3) leads to a spurious strain as

$$\hat{\varepsilon}_x = \cos\theta - 1 + \frac{1}{2}\sin^2\theta \neq 0$$

The spurious strain will become zero only if we assume the rigid body rotation is small, such that:

$$\cos\theta \approx 1 - \frac{1}{2}\theta^2, \qquad \sin\theta \approx \theta$$

then the approximation becomes

$$\hat{\varepsilon}_x = \cos\theta - 1 + \frac{1}{2}\sin^2\theta \approx -\frac{1}{2}\theta^2 + \frac{1}{2}\theta^2 = 0$$

Thus, it is clear that this simple FE approximation is valid only for the small rotation or small increment if the large rigid body rotation is analyzed by an incremental solution. In addition to the large 2D rigid rotation, the problem is further complicated by the fact that large 3D rotations of the cable do not possess vector properties, as in the case of infinitesimal rotations. However, one can always calculate the strain correctly by directly comparing the element's current length (using element position vector) with its original length without using the displacement approach.

Advanced techniques to parameterize large 3D rotations are developed in the finite element approximation. These include Euler angles [12], Euler parameters, Rodrigues parameters or semi-tangential rotations [13, 14], Quaternion algebra [15], conformal rotation vector [16], rotational vector [17] and co-rotational formulation [18]. These techniques address the large rigid body rotation mentioned above with more accurate formulation and allow a much large rotation increment in an incremental solution. However, over a very long period time of simulation of flexible member such as cable, the accumulated error may lead to spurious energy increase in the simulated system resulting in numerical instability. The error in strain energy is mainly due to the existing FE methods calculating the strain energy by nodal displacements where the displacements caused by the large rigid body rotation is decoupled from the small elastic stretch of the cable approximately. Advanced energy-conserving FE method [19] has been developed to specially address the flexible member experiencing the large rigid body rotation. These existing efforts represent substantial and novel contributions in FE modeling of flexible member; however, their formulations are mathematically more complicated than the FD method used in the field.

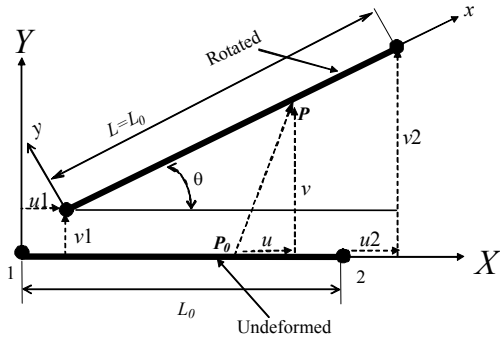

Figure 1. Cable element in large rigid body rotation.

The current study is motivated by the need of a simple and robust finite element method for the dynamic analysis of towed cables. As demonstrated above, the simple FE approximation, based on nodal displacement formulation, is problematic in dealing with the large rigid body displacements and rotations and more advanced and accurate FE approximation formulations are needed. However, these advanced formulations are usually more complex than the FD methods used in the field. To take FE's advantage in modeling flexibility and FD's advantage in simplicity, an alternative finite element method has been developed by solving for the position vector of an element directly instead of the nodal displacements first in order to obtain the new position of the element indirectly. Thus, the position vector finite element method will (i) have no limitation in dealing with the large rigid body rotations, and (ii) eliminate the approximation and accumulation errors in strain energy of simulated system arising from the incremental solution process by comparing the current configuration of element (through nodal position) with its original configuration directly. In addition, the formulation of the position vector finite element method is simple and straightforward, especially in dealing with the external loads such as drag. The newly derived position vector finite element method has been validated by experiments including sea trials.

2. POSITION VECTOR FINITE ELEMENT METHOD

Consider a two-noded straight cable element in a three-dimensional space. The element geometry is described by its nodal coordinates (X_i, Y_i, Z_i) (i = 1, 2) in the global coordinate system *OXYZ*. Local coordinates x, y and z are defined with x-axis along the cable, y and z perpendicular to the x-axis, respectively.

Assume the coordinates of an arbitrary point along the cable element is expressed in terms of element shape functions and nodal coordinates, such that:

$$\boldsymbol{R} = \boldsymbol{N}\boldsymbol{X}_e \tag{4}$$

where $\boldsymbol{R} = \{X, Y, Z\}^T$ is the global position vector of the arbitrary point, $\boldsymbol{X_e} = \{X_1, Y_1, Z_1, X_2, Y_2, Z_2\}^T$ is the global nodal coordinates and $\boldsymbol{N}$ is the element shape functions. In this application, the linear shape functions are used for the cable element, such as,

$$\boldsymbol{N} = \begin{bmatrix} N_1(\xi) & 0 & 0 & N_2(\xi) & 0 & 0 \\ 0 & N_1(\xi) & 0 & 0 & N_2(\xi) & 0 \\ 0 & 0 & N_1(\xi) & 0 & 0 & N_2(\xi) \end{bmatrix} \tag{5}$$

where

$$N_1(\xi) = 1-\xi, \quad N_2(\xi) = \xi, \quad \xi = x/L$$

$$L = \sqrt{(X_2 - X_1)^2 + (Y_2 - Y_1)^2 + (Z_2 - Z_1)^2}$$

and L is the current length of the cable element.

Similarly, the velocity and acceleration of the element will be interpolated by the same element shape functions such that:

$$\boldsymbol{v} = \dot{\boldsymbol{R}} = \boldsymbol{N}\dot{\boldsymbol{X}}_e, \text{ and } \boldsymbol{a} = \ddot{\boldsymbol{R}} = \boldsymbol{N}\ddot{\boldsymbol{X}}_e \tag{6}$$

where $\boldsymbol{v} = \{v_x, v_y, v_z\}^T$ and $\boldsymbol{a} = \{a_x, a_y, a_z\}^T$ are the global velocity and acceleration vectors of the arbitrary point.

The deformation of the cable element is defined as:

$$u = x - x_0 = \xi(L - L_0) \tag{7}$$

where x_0 and x are the coordinates of an arbitrary point along the element before and after deformation and L_0 is the length of undeformed element.

The Green-Lagrangian strain of the element is defined as:

$$\begin{aligned} \varepsilon_x &= \frac{L}{L_0} - 1 \\ &= \frac{X_2 - X_1}{L_0}\cos\theta_x + \frac{Y_2 - Y_1}{L_0}\cos\theta_y + \frac{Z_2 - Z_1}{L_0}\cos\theta_z - 1 \\ &= \boldsymbol{B}\boldsymbol{X}_e - 1 \end{aligned} \tag{8}$$

where the directional cosines are defined as:

$$cos\,\theta_x = \frac{X_2 - X_1}{L} \quad cos\,\theta_y = \frac{Y_2 - Y_1}{L} \quad cos\,\theta_z = \frac{Z_2 - Z_1}{L} \tag{9}$$

and $\boldsymbol{B}$ is the strain matrix, such that:

$$\boldsymbol{B} = \left[-\frac{cos\,\theta_x}{L_0}, -\frac{cos\,\theta_y}{L_0}, -\frac{cos\,\theta_z}{L_0}, \frac{cos\,\theta_x}{L_0}, \frac{cos\,\theta_y}{L_0}, \frac{cos\,\theta_z}{L_0} \right] \tag{10}$$

The strain matrix $\boldsymbol{B}$ can be further decomposed into the product of the strain matrix in the local coordinates of element $\boldsymbol{B_0}$ and the coordinate transformation matrix $\boldsymbol{Q}$, such as:

$$\boldsymbol{B} = \boldsymbol{B_0}\boldsymbol{Q} \tag{11}$$

where

$$\boldsymbol{B_0} = \left[-\frac{1}{L_0}, \ 0, \ 0, \ \frac{1}{L_0}, \ 0, \ 0 \right]$$

$$\boldsymbol{Q} = \begin{bmatrix} \cos\theta_x & \cos\theta_y & \cos\theta_z & 0 & 0 & 0 \\ 0 & 0 & 0 & 0 & 0 & 0 \\ 0 & 0 & 0 & 0 & 0 & 0 \\ 0 & 0 & 0 & \cos\theta_x & \cos\theta_y & \cos\theta_z \\ 0 & 0 & 0 & 0 & 0 & 0 \\ 0 & 0 & 0 & 0 & 0 & 0 \end{bmatrix}$$

It should be noted that local strain matrix $\boldsymbol{B_0}$ is the same as the existing finite element method.

2.1 Mass Matrix

The mass matrix is derived from the kinetic energy of the element, such that:

$$T = \frac{1}{2}\int_0^L \rho A \dot{\boldsymbol{R}} \cdot \dot{\boldsymbol{R}} dx = \frac{1}{2}\dot{\boldsymbol{X}}_e^T \boldsymbol{M}\dot{\boldsymbol{X}}_e \tag{12}$$

where $\boldsymbol{M}$ is the mass matrix of the cable element

$$\boldsymbol{M} = \frac{\rho AL}{6}\begin{bmatrix} 2 & 0 & 0 & 1 & 0 & 0 \\ 0 & 2 & 0 & 0 & 1 & 0 \\ 0 & 0 & 2 & 0 & 0 & 1 \\ 1 & 0 & 0 & 2 & 0 & 0 \\ 0 & 1 & 0 & 0 & 2 & 0 \\ 0 & 0 & 1 & 0 & 0 & 2 \end{bmatrix}$$

In the above equation, ρ and A are the material density and cross section area of the cable element, respectively. It should be noted that the element mass matrix is constant in the global coordinate system.

2.2 Stiffness Matrix

The stiffness matrix can be derived from the strain energy of the element, such that:

$$U = \frac{1}{2}\int_0^L EA\varepsilon_x^2 dx = \frac{1}{2}\boldsymbol{X}_e^T\boldsymbol{K}\boldsymbol{X}_e - \boldsymbol{X}_e^T\boldsymbol{F}_k + \frac{1}{2}EAL \tag{13}$$

where E is Young's modulus of the cable element, $\boldsymbol{K}$ is the stiffness matrix of the element and $\boldsymbol{F_k}$ is the generalized nodal force vector resulting from the elasticity of the cable element, such as:

$$\boldsymbol{K} = EAL\boldsymbol{B}^T\boldsymbol{B} = \boldsymbol{Q}^T\boldsymbol{K_0}\boldsymbol{Q}$$

$$\boldsymbol{K_0} = EAL\boldsymbol{B_0}^T\boldsymbol{B_0} = \frac{EAL}{L_0^2}\begin{bmatrix} 1 & 0 & 0 & -1 & 0 & 0 \\ 0 & 0 & 0 & 0 & 0 & 0 \\ 0 & 0 & 0 & 0 & 0 & 0 \\ -1 & 0 & 0 & 1 & 0 & 0 \\ 0 & 0 & 0 & 0 & 0 & 0 \\ 0 & 0 & 0 & 0 & 0 & 0 \end{bmatrix}$$

$$\boldsymbol{F_k} = EAL\boldsymbol{B}^T = EAL\boldsymbol{Q}^T\boldsymbol{B_0}^T$$

Note $\boldsymbol{F_k}$ does not exist in existing FE methods. For small strain deformations, $L/L_0 = 1+\varepsilon_x \approx 1$. Then, the matrix $\boldsymbol{K_0}$ is simplified to the stiffness matrix of the existing cable element. The $\boldsymbol{K}$ and $\boldsymbol{F_k}$ are highly nonlinear and time-dependant as the coordinate transformation matrix $\boldsymbol{Q}$ is the function of the orientation of the cable element that varies in time. It should be noted that the stiffness matrix $\boldsymbol{K}$ of the position vector FE method does not decouple into the linear and nonlinear geometric stiffness matrices because it calculates the strain directly from position vector instead of displacement.

2.3 Material Viscous Damping Matrix

The material damping effect of the cable is assumed as viscous damping, such that:

$$\sigma_v = -c\dot{\varepsilon}_x = -c\boldsymbol{B}\dot{\boldsymbol{X}}_e \tag{14}$$

where c is the viscous damping coefficient.

Then the virtual work done by the viscous damping force is given by:

$$\delta W_v = \int_0^L EA\sigma_v\delta\varepsilon_x dx = -c\delta\boldsymbol{X}_e^T\boldsymbol{K}\dot{\boldsymbol{X}}_e = -\delta\boldsymbol{X}_e^T\boldsymbol{C}\dot{\boldsymbol{X}}_e \tag{15}$$

where $\boldsymbol{C} = c\boldsymbol{K}$ is the viscous damping matrix, $\boldsymbol{K}$ is the stiffness matrix of the cable element defined in Eq. (13) and δ is the variational operator, respectively.

2.4 Fluid Dynamic Force Vectors

For the application in towed cables, the fluid dynamic effects of the drag and added mass must be included [20]:

$$\boldsymbol{f_{dn}} = -C_{dn}(\alpha)\frac{\rho_0 D}{2}V^2\frac{\boldsymbol{V_n}}{|\boldsymbol{V_n}|} \tag{16a}$$

$$\boldsymbol{f_{dt}} = -C_{dt}(\alpha)\frac{\rho_0 D}{2}V^2\frac{\boldsymbol{V_t}}{|\boldsymbol{V_t}|} \tag{16b}$$

$$\boldsymbol{f_a} = -C_m\rho_0 A\dot{\boldsymbol{V}}_n \tag{16c}$$

$$\boldsymbol{V} = \dot{\boldsymbol{R}} - \boldsymbol{V_c} \qquad \boldsymbol{V_n} = (\boldsymbol{I} - \boldsymbol{k_0})\cdot\boldsymbol{V} \qquad \boldsymbol{V_t} = \boldsymbol{k_0}\cdot\boldsymbol{V} \tag{16d}$$

where $\boldsymbol{f_{dn}}$ and $\boldsymbol{f_{dt}}$ are the drag forces normal and tangent to the element, $C_{dn}(\alpha)$ and $C_{dt}(\alpha)$ are the normal and tangent loading functions of the drag, α is the angle of attack, ρ_0 is the fluid density, D is the cable diameter, $\boldsymbol{f_a}$ is the inertial force normal to the element resulting from the added mass of fluid surrounding the element, C_m is the added mass coefficient of the element, $\boldsymbol{I}$ is the unit matrix, and $\boldsymbol{V_c}$ is the free stream velocity of the fluid, respectively.

The virtual work done by the inertial force of the added mass effect is given by:

$$\delta W_a = \int_0^L \boldsymbol{f_a}\cdot\delta\boldsymbol{R}dx = -\delta\boldsymbol{X}_e^T\boldsymbol{M_a}\ddot{\boldsymbol{X}}_e + \delta\boldsymbol{X}_e^T\boldsymbol{F}_a \tag{17}$$

where $\boldsymbol{M_a}$ is the added mass matrix resulting from the fluid surrounding the element, and $\boldsymbol{F_a}$ is the inertial force due to the added mass of the fluid surrounding the element, respectively. In the above equation, the added mass matrix and the inertia force vector are given by:

$$\boldsymbol{M_a} = \frac{C_m\rho_0 AL}{6}(\boldsymbol{M_{a0}} - \boldsymbol{M_{a1}}) \tag{18a}$$

$$\boldsymbol{M_{a0}} = \begin{bmatrix} 2\boldsymbol{I}_{3\times3} & \boldsymbol{I}_{3\times3} \\ \boldsymbol{I}_{3\times3} & 2\boldsymbol{I}_{3\times3} \end{bmatrix} \qquad \boldsymbol{M_{a1}} = \begin{bmatrix} 2\boldsymbol{m_0} & \boldsymbol{m_0} \\ \boldsymbol{m_0} & 2\boldsymbol{m_0} \end{bmatrix} \tag{18b}$$

$$\boldsymbol{m_0} = \begin{bmatrix} \cos^2\theta_x & \cos\theta_x\cos\theta_y & \cos\theta_x\cos\theta_z \\ \cos\theta_x\cos\theta_y & \cos^2\theta_y & \cos\theta_y\cos\theta_z \\ \cos\theta_x\cos\theta_z & \cos\theta_z\cos\theta_y & \cos^2\theta_z \end{bmatrix} \tag{18c}$$

$$\boldsymbol{F_a} = \boldsymbol{M_a}\dot{\boldsymbol{V}}_c^e \tag{18d}$$

where $\boldsymbol{I}_{3\times3}$ is the unity matrix of 3 by 3, and $\dot{\boldsymbol{V}}_c^e = \left(V_{cx1}^e,\ V_{cy1}^e,\ V_{cz1}^e,\ V_{cx2}^e,\ V_{cy2}^e,\ V_{cz2}^e\right)^T$ is the fluid acceleration vector at the element nodes. It should be noted that both the added mass matrix and the inertial force vector are highly nonlinear and time dependent as the element's orientation varies in time.

The drag forces will be calculated in the local element coordinates. Assume the local coordinate system is constructed in a such way that the x-axis is aligned with the cable element, the y-axis is aligned in the plane containing the x-axis and the relative fluid velocity vector but normal to the element, and the

z-axis is the cross product of x and y. Thus, the fluid velocity relative to the element in the local coordinates can be expressed as:

$$\boldsymbol{v} = \dot{\boldsymbol{r}} - \boldsymbol{v}_c = \left(\dot{x} - v_{cx},\quad \dot{y} - v_{cy},\quad 0\right)^T \tag{19}$$

where $\boldsymbol{r}$ and $\boldsymbol{v_c}$ are the position vectors of an arbitrary point along the cable element and the fluid velocity in local coordinates, respectively. Assume the position vector $\boldsymbol{r}$ and the fluid velocity $\boldsymbol{v_c}$ are interpolated by the same element shape functions in Eq. (5), such that,

$$\boldsymbol{r} = \boldsymbol{N}\boldsymbol{x_e},\qquad \boldsymbol{v_c} = \boldsymbol{N}\boldsymbol{v_c^e} \tag{20}$$

where $\boldsymbol{x_e}$ = (x_{e1}, y_{e1}, z_{e1}, x_{e2}, y_{e2}, z_{e2})^T is the local nodal coordinate vector of element and $\boldsymbol{v_c^e}$ = (v_{cx1}, v_{cy1}, v_{cz1}, v_{cx2}, v_{cy2}, v_{cz2})^T is the vector of fluid velocity at the element nodes in local coordinates, respectively.

From Eq. (16a,b), the drag force vector in the local coordinates can be expressed as:

$$\boldsymbol{f_d} = \frac{\rho_0 D}{2} v^2 \left\{-C_{dt}(\alpha)\text{sign}(v_x),\quad -C_{dn}(\alpha)\text{sign}(v_y),\quad 0\right\} \tag{21}$$

Therefore, the virtual work done by the drag forces is given by:

$$\delta W_d = \int_0^L \boldsymbol{f_d}\cdot\delta\boldsymbol{r}\,dx = -\delta\boldsymbol{x_e}^T\boldsymbol{f_d^e} \tag{22}$$

where $\boldsymbol{f_d^e}$ is the equivalent nodal drag forces in the local coordinates, such that:

$$\boldsymbol{f_d^e} = \begin{Bmatrix} C_{dt}(\alpha)\dfrac{\rho_0 D}{2}\text{sign}(v_x)f_1 \\ C_{dn}(\alpha)\dfrac{\rho_0 D}{2}\text{sign}(v_y)f_1 \\ 0 \\ C_{dt}(\alpha)\dfrac{\rho_0 D}{2}\text{sign}(v_x)f_2 \\ C_{dn}(\alpha)\dfrac{\rho_0 D}{2}\text{sign}(v_y)f_2 \\ 0 \end{Bmatrix}$$

$$f_i = \dot{\boldsymbol{x}}_e^T\cdot\boldsymbol{A}_i\cdot\dot{\boldsymbol{x}}_e - 2\dot{\boldsymbol{x}}_e^T\cdot\boldsymbol{A}_i\cdot\boldsymbol{v}_e + \boldsymbol{v}_e^T\cdot\boldsymbol{A}_i\cdot\boldsymbol{v}_e \qquad (i = 1, 2)$$

$$A_1 = \frac{1}{12}\begin{bmatrix} 3&0&0&1&0&0\\ 0&3&0&0&1&0\\ 0&0&3&0&0&1\\ 1&0&0&1&0&0\\ 0&1&0&0&1&0\\ 0&0&1&0&0&1 \end{bmatrix} \quad A_2 = \frac{1}{12}\begin{bmatrix} 1&0&0&1&0&0\\ 0&1&0&0&1&0\\ 0&0&1&0&0&1\\ 1&0&0&3&0&0\\ 0&1&0&0&3&0\\ 0&0&1&0&0&3 \end{bmatrix}$$

Note that the drag force vector is a nonlinear function of the unknown nodal velocity $\dot{\boldsymbol{x}}_e$ of the element.

Finally, the equivalent nodal drag force vector in the global coordinates is obtained by the coordinate transformation, such that:

$$\boldsymbol{F_d} = \boldsymbol{T}^T\boldsymbol{f_d^e} \tag{23}$$

where $\boldsymbol{T^T}$ is the coordinate transformation matrix from the local coordinates to the global coordinates systems.

2.7 Buoyant and Gravity Force Vector

Assume the buoyant force is given in the global coordinates, such as:

$$\boldsymbol{f_{bg}} = \{0,\ 0,\ -A(\rho - \rho_0)g\}^T \tag{24}$$

where A is the cross section area of the element, ρ and ρ_0 are the densities of material and fluid, and g is the acceleration due to gravity, respectively.

Accordingly, the virtual work done by the force is:

$$\delta W_{bg} = \int_{0e}^{L} A\rho_0\boldsymbol{f_{bg}}\cdot\delta\boldsymbol{R}\,dx = \delta\boldsymbol{X}_e^T\boldsymbol{F_b} \tag{25}$$

where $\boldsymbol{F_{bg}}$ is the equivalent nodal buoyant force vector, such that:

$$\boldsymbol{F}_{bg} = \int_0^L A\rho_0\boldsymbol{N}^T\cdot\boldsymbol{f_b}\,dx = -\frac{LA(\rho-\rho_0)g}{2}\{0,0,1,0,0,1\}^T$$

The expression of the equivalent nodal buoyant and gravity force vectors is constant in the global coordinate system.

2.8 Equation of Motion

The equation of motion is derived from the principle of virtual work in dynamics, such that:

$$\delta U - \delta T - \delta W_v - \delta W_a - \delta W_d - \delta W_{bg} = 0 \tag{26}$$

Substituting Eqs. (12,13,15,22,25) into Eq. (42) leads to the equation of motion as:

$$\left[\boldsymbol{M} + \boldsymbol{M_a}\right]\ddot{\boldsymbol{X}}_e + \boldsymbol{C}\dot{\boldsymbol{X}}_e + \boldsymbol{K}\boldsymbol{X}_e = \boldsymbol{F_k} + \boldsymbol{F_a} - \boldsymbol{F_d} + \boldsymbol{F_{bg}} \tag{27}$$

The equation of motion in Eq. (27) is highly nonlinear because the matrices of added mass, damping, and stiffness on the left hand side and the force vectors of on the right are the functions of the current position $\boldsymbol{X_e}$ and its velocity $\dot{\boldsymbol{X}}_e$.

3. VALIDATION AND APPLICATION

The newly derived position vector finite element method for the cable dynamics has been implemented into a computer program and the 4th order Runge-Kutta numerical integrator is adopted to solve the equation of motion numerically. The program has been validated with laboratory experiments and sea trials of real towed cable system.

3.1 Submerged Cable Snapping in Water

An experimentally examined submerged cable system [21] was investigated to validate the applicability and robustness of the position vector finite element method. The system consisted of a steel aircraft type cable with a spherical payload attached at the cable's lower end. The system was excited by a sinusoidal motion at the top support of the cable. Table 1-2 give the parameters of the cable and the payload. The cable was modeled by five cable elements with equal length while the payload was modeled as a lumped mass element. The time integration step was Δt = 0.05s. The cable tension responses at

the upper support to the external excitation with different frequencies were analyzed. Figure 2 shows the cable tensions at the top end when the exciting frequency was less than the natural frequency of the submerged cable system. The results are normalized by the static tension T_0. Compared with the experimental data, the simulated cable tension agrees with the experimental data very well. As the frequency of excitation approaches the natural frequency of the submerged cable system, the cable experiences a transition from being slack to being taut as shown in Fig.3. The simulation results agree with the experimental data well even in this unstable condition. It demonstrates that the newly derived position vector finite element method is robust and accurate.

Table 1. Mechanical properties of cable specimen.

Diameter (mm)	Length (m)	No. of Strands	Density (kg/m)	Rigidity *EA* (kN)	Drag Coeff.	
					C_{dn}	C_{dt}
1.6	18.9	7x7	0.0112	134.2	1.2	0.01

Table 2. Mechanical properties of payload sphere.

Diameter (mm)	Mass (kg)	Drag Coeff. C_d	Added Mass Coeff. C_a
203.2	12.2	0.5	0.18

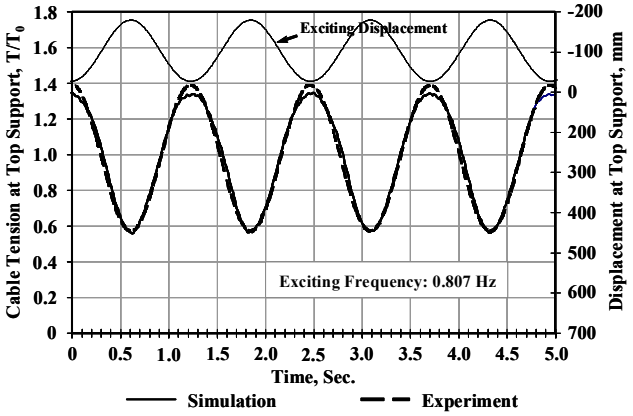

Figure 2. Tension at frequency, *f* = 0.807 Hz.

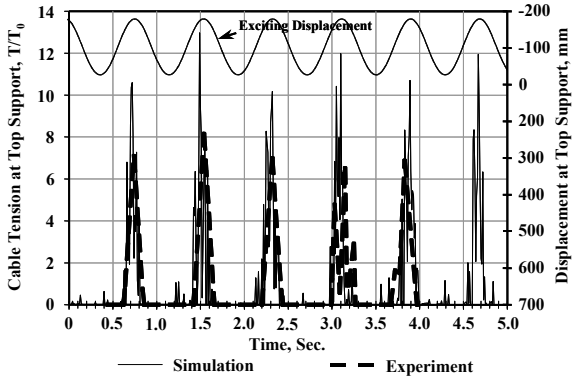

Figure 3. Tension at resonant frequency, *f* = 1.27 Hz.

3.2 Submerged Cable and Towed-Body System

Consider a submerged cable and towed-body system towed by a surface ship tested in a sea trial. The cable and body were towed at 22.2 *km/h* (12 knots) speed while the ship executed a 270 degree turn. The total cable length was 460 m with 125 m fairing cable at the bottom and 355 m bare cable at the top. The drag loading functions of the bare cable are given in Eq. (28):

$$C_{Dt} = D_0\left(-0.019 + 0.0239\cos\alpha + 0.02\sin\alpha + 0.001\cos 2\alpha\right)$$
$$C_{Dn} = D_0 \sin^2\alpha \qquad (28)$$

while the drag loading functions of the fairing cable are given in Eq. (29):

$$\left.\begin{array}{l} C_{Dt} = D_0\left(0.273 + 0.827\alpha^2\right)\cos\alpha \\ C_{Dn} = D_0\left(0.273 + 0.827\alpha^2\right)\sin\alpha \end{array}\right\} \; 0^\circ \le \alpha < 30^\circ$$
$$\left.\begin{array}{l} C_{Dt} = D_0 \sin\alpha\cos\alpha \\ C_{Dn} = D_0 \sin^2\alpha \end{array}\right\} \; 30^\circ \le \alpha \le 90^\circ \qquad (29)$$

The bare cable was divided into nine equally spaced elements while the fairing cable was divided into three equally spaced elements. The towed-body was modeled as a rigid body. Tables 3 and 4 show the parameters of the cable and towed body system. Measured ship motion at the towing point was used as an input to the cable and towed-body system. Figure 4 shows the measured ship trajectory (thick line) together with the simulated body's trajectory (thin line) in the horizontal plane. The towed body followed the ship's trajectory very closely as expected. The simulated time history of body's depth was then compared with the measured data in Fig. 5. Good agreement is observed between the simulation and the trial data.

Table 3. Parameters of cable.

Cable Type	Diameter (*m*)	Density (*kg/m*)	Drag D_0	Elasticity *EA* (*kN*)
Bare	0.0411	5.20	1.70	2.625×10^4
Fairing	0.0800	8.32	0.15	

Table 4. Parameters of towed body.

Mass (*kg*)	9,500	I_{xx} (kgm^2) – Forward	3,804
Volume (m^3)	6.25	I_{yy} (kgm^2) – Side	10,363
Length (*m*)	3.81	I_{zz} (kgm^2) – Downward	8,375

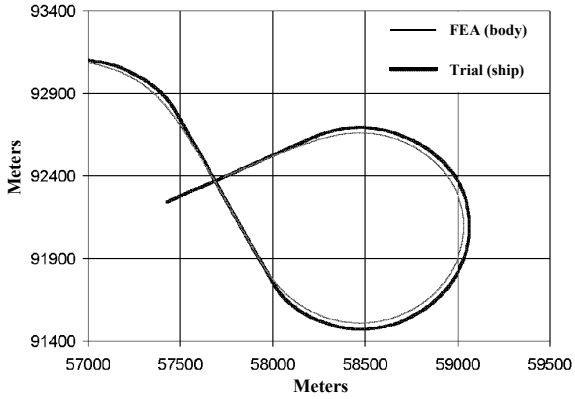

Figure 4. Horizontal trajectories of ship and body.

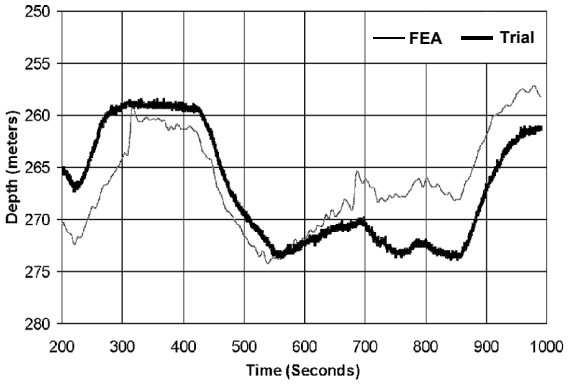

Figure 5. Time history of towed body's depth.

CONCLUSION

This paper presents an alternative finite element method to model the dynamics of towed cable system. It is formulated in terms of element nodal position instead of nodal displacement used in the existing FE methods, in order to take FE's advantage in modeling flexibility and FD's advantage in simplicity as well as to eliminate the accumulated errors arising from existing FE methods that solve for displacements first in order to obtain the cable position over very long period of time. Simulation results show that this newly derived FE method is simple, robust, and effective as seen in comparisons with experimental and sea trial data.

ACKNOWLEDGMENTS

This work was supported by the Ontario Centres of Excellence, Ontario, Canada and Curtiss-Wright Controls, Engineered Systems - Marine Defense.

REFERENCES

[1] Dessi, D., Carcaterra, A., D. Diodati, 2004, "Experimental investigation versus numerical simulation of the dynamic response of a moored floating structure to waves", *Journal of Engineering for the Maritime Environment*, Vol **218 (M3)**, pp. 153-165.

[2] Prabhakar, S., B. Buckham, 2005, "Dynamics modeling and control of a variable length remotely operated vehicle tether", OCEANS 2005, Vol **2**, pp. 1255-1262.

[3] Vassberg, J. C., Yeh, D. T., Blair, A. J. and Evert, J. M., 2002, "Dynamic Characteristics of a KC-10 Wing-Pod Refueling Hose by Numerical Simulation," *20th AIAA Applied Aerodynamics Conference*, AIAA 2002-2712.

[4] Padgett, D.A., A.P. Mazzoleni, 2007, "Nullcline analysis as an analytical tethered satellite mission design tool", *J Guid Control Dynam*, Vol **30(3)**, pp. 741-752.

[5] Zhu Z.H., Maguid S.A., L.S. Ong, 2003, "Dynamic multiscale simulation of towed cable and body", *The Second MIT conference on Computational Fluid and Solid Mechanics*, Paper No. 521, Cambridge, USA (June 2003).

[6] Eames M.C., 1967, "Steady-State Theory of Towing Cables", *Defence Research Establishment Atlantic, Canada*, DREA Report 67/5.

[7] Buckham B. and M. Nahon, 1999, "Dynamics Simulation of Low Tension Tethers", *OCEANS'99 MTS/IEEE*, Seattle, USA, pp. 757-766.

[8] Koh C.G., Zhang Y., S.T. Quek, 1999, "Low-tension Cable Dynamics: Numerical and Experimental Studies", *J Eng Mech-ASCE*, Vol **125** (3), pp. 347-354.

[9] Lalu, P.P., 2007, "Numerical simulation of two-part underwater towing system a lumped mass-spring system approach", OMAE2007, Vol **4**, pp. 387-390.

[10] Burgess J.J., 1992, "Equations of Motion of a Submerged Cable with Bending Stiffness", *Offshore Marine and Arctic Engineering*, **Vol** 1-A, pp. 283-289.

[11] Fung Y.C., 1993, *First Course in Continuum Mechanics*, 3 edition, Prentice Hall, USA.

[12] Stuelpnagel J., 1964, "On the Parameterization of Three-dimensional rotation Group", *SIAM Review*, Vol **6**, pp. 422-430.

[13] Argyris J.H., 1982, "An Excursion into Large Rotations", *Comput Method Appl M*, Vol **32**, pp. 85-155.

[14] Besseling J.F., 1985, "Large rotations in problems of structural mechanics, in finite element methods for nonlinear problems", *Proc. Europe-US symposium*, Trondheim, Norway, pp. 25-39.

[15] Spring K.W., 1986, "Euler Parameters and The Use of Quaternion Algebra in the Manipulation of finite Rotations: A Review", *Mech Mach Theory*, Vol **21(5)**, pp. 365-373.

[16] Milenkovic V., "Coordinates suitable for angular motion synthesis in robots", *Proc. ROBOT 6 conference*, 1982.

[17] Cardona A., M. Geradin, 1988, "A Beam Finite element Non-linear Theory with Finite Rotations", *Int J Numer Meth Eng*, Vol **26**, pp. 2403-2438.

[18] Crisfield M.A., 1990, "A Consistent Co-rotational Formulation for Non-linear Three-dimensional Beam elements", *Comput Method Appl M*, Vol **81**, pp. 131-150.

[19] Simo, J.C., Posbergh, T.A. 1988, "Nonlinear dynamics of flexible structures: geometrically exact formulation and stability", *Proc. of 27 IEEE Conference*, Vol **2**, pp. 1732-1737.

[20] Zhu Z.H. and Meguid S.A., 2006, "Elastodynamic Analysis of Aerial Refueling Hose Using Curved Beam", *AIAA J*, **Vol** 44(6), pp. 1317-1324.

[21] Geoller J.E., 1969, "A Theoretical and Experimental Investigation on Snap Loads in Stranded Steel Cables", NOLTR 69-215, US Naval Ordance Laboratory, White Oak, Maryland, USA (1969).

CURTISS-WRIGHT

Info

curtisswrightds.com

Email

ds@curtisswright.com